

Experimental identification of the shear failure modes of a voided precast wall element subjected to lateral loading

B. Dal Lago¹, M. Del Galdo², A. Dal Lago³, L. Ferrara⁴

ABSTRACT: The paper describes the experimental results and the engineering interpretation of shear tests carried out at Politecnico di Milano on precast concrete wall elements characterised by inner lightening cavities contoured by a solid frame. At the base of the solid columns mechanical devices connect the wall element with the lower element or with the foundation. The presence of the lightening cavities does not allow for a clear collocation within the classical structural behaviour of walls or frames. This activity frames into a wider research program focused on an innovative dry-assembled precast system for residential constructions named Domus Dry® patented by DLC Consulting srl of Milan and received main funding from the programme “Brevetti+” (GU 179 02/08/2011). An experimental programme was carried out at the Laboratorio Prove Materiali Strutture e Costruzioni - Politecnico di Milano with the aim of characterising the shear behaviour of the wall under different reinforcement layouts: five full-scale wall specimens reinforced with different layouts were subjected to monotonic and cyclic testing through the application of a horizontal displacement history. Different failure modes corresponded to different reinforcement layouts. Failure in tension-shear was identified for weakly reinforced walls, whilst sliding-shear failure was identified for heavily reinforced walls. The tensile testing of the wall vertical joint performed within the global wall test configuration showed a satisfactory behaviour of the connection. A structural strut & tie modelling of the wall elements has been set to provide an engineering interpretation of the experimental results.

1 INTRODUCTION

Precast concrete wall structures are diffused throughout the world for the construction of residential buildings. The present paper reports about cyclic testing of single wall elements with different reinforcement layouts assembled to their foundation and subjected to lateral loading. The wall element under investigation belongs to an innovative construction system named Domus® conceived by DLC Consulting srl (Dal Lago, 2002, 2006), later modified into Domus Dry® (Dal Lago, 2012a and Dal Lago *et al.*, 2016). The wall element of this system is internally lightened through vertical cavities or polystyrene blocks. Hollow precast walls have been introduced in the literature mainly with reference to hollow core panels (Bora *et al.* 2007, Hamid and Mander 2010, Chu *et al.* 2017, Xiong *et al.* 2018, Xu and Li 2019). The wall under consideration has been previously subjected to a full-scale experimental programme within the Safecast project (Negro *et al.*, 2013) which allowed the characterisation of its structural behaviour in bending (Dal Lago *et al.*, 2017). This paper deals with the assessment of the shear strength and failure modes of this structural wall system.

2 WALL SPECIMENS

Four wall specimens have been designed and casted to carry out the experimental programme. All of them are provided with internal vertical prismatic cavities made with polystyrene blocks. It has to be noted that the cavities are intended to be hollow, but these elements have not been produced using the sophisticated vertical moulds needed for this purpose (Dal Lago and Dal Lago, 2018). At the edges of the lightening blocks, the wall element is characterised by a solid monolithic portal frame which is braced by the two

¹ Adjunct Professor, Politecnico di Milano, Italy, brunoalberto.dallago@polimi.it

² Professional Engineer, DLC Consulting S.r.l., m.delgaldo@dlc-consulting.it

³ President, DLC Consulting S.r.l., a.dallago@dlc-consulting.it

⁴ Associate Professor, Politecnico di Milano, liberato.ferrara@polimi.it

concrete layers on either side (Figure 1a). At the bases of the columns of the equivalent portal frame, an innovative mechanical device called Kaptor is installed to connect the same wall panel to the lower wall element or to the foundation (Figure 1b). The employed version of the Kaptor device is made by two thick steel plates with a central hole aimed to be inserted into the protruding bar anchors left in the element below. The longitudinal reinforcing bars are connected to the plates through a threading made on the terminal bar portion after upset treatment. Additional arched-shaped bars are welded to the plates, intended to compensate the concrete volume reduction due to the one-side only recesses necessary to screw the nuts into the bolts. The device can be classified as an over-designed coupler, conceived according to capacity design to allow for the full development of plasticity and failure into the longitudinal rebars. The device used is an evolution of the original one developed about 10 years ago (Dal Lago, 2012, Dal Lago *et al.*, 2016).

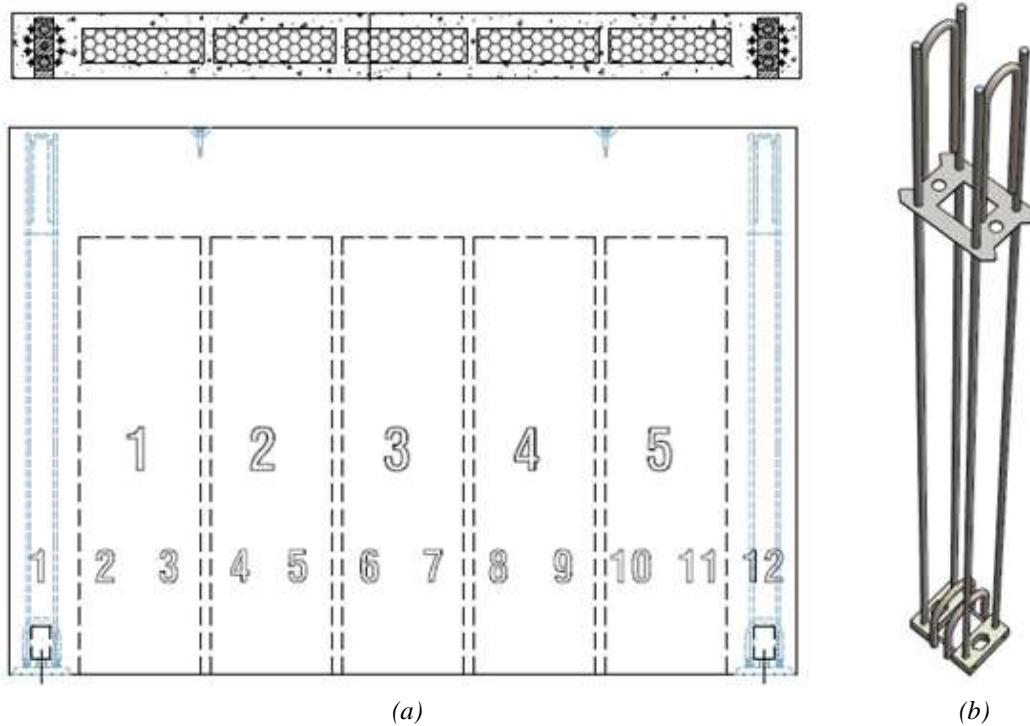


Figure 1. (a) Schematic geometry of the wall elements with internal prismatic lightening; (b) Kaptor connection element in the lateral plain portions of the wall.

The geometry and the schematic reinforcement details of the different wall specimens are shown in Figure 2. The longitudinal reinforcement is made with 4 $\phi 16$ rebars connected to 2 Kaptor devices at each wall column. Wall 1 is a fictitious $4.8 \times 2.5 \times 0.25$ m wall element where no reinforcement at all is inserted into the shear-resistant concrete layers external to the lightening cavities (Figure 2a). The thickness of the external layers is $50 + 50$ mm. Wall 2 has the same geometry and reinforcement of Wall 1 plus two $\phi 8/15$ welded wire meshes used to reinforce the central panel area, one per concrete layer (Figure 2b). Wall 3 is a $3.6 \times 2.5 \times 0.30$ m wall element where, besides the two $\phi 8/150$ welded wire meshes, 16 $\phi 10$ bars are placed diagonally (4 bars per diagonal per each concrete layer) to improve the shear strength of the panel (Figure 2c). The thickness of the external layers is $7.5 + 7.5$ cm. Wall 4 has the same geometry and reinforcement of Wall 3 plus the installation of 60 cm long debonding sleeves over all the longitudinal rebars right above the Kaptor connection which are intended to increase the plasticisation length and, therefore, ductility and dissipation of energy in bending. Walls 3 and 4 are shorter and have higher shear reinforcement, since they have been over-designed for tension-shear strength with respect to bending strength.

The foundation is an inverted T-shaped precast concrete beam. Each foundation is reinforced with $2\phi 12$ at the superior. Stirrups are $\phi 8/20$. The threaded anchors are 4 M27 with end nail-head enlargement, two at each edge of the foundation, protruding 140 mm from the foundation extrados and embedded for 525 mm into it.

The connection is assembled following the next steps (Figure 3): (I) screwing of the lower shallow nut on the anchor; (II) positioning of the wall; (III) partial screwing of the

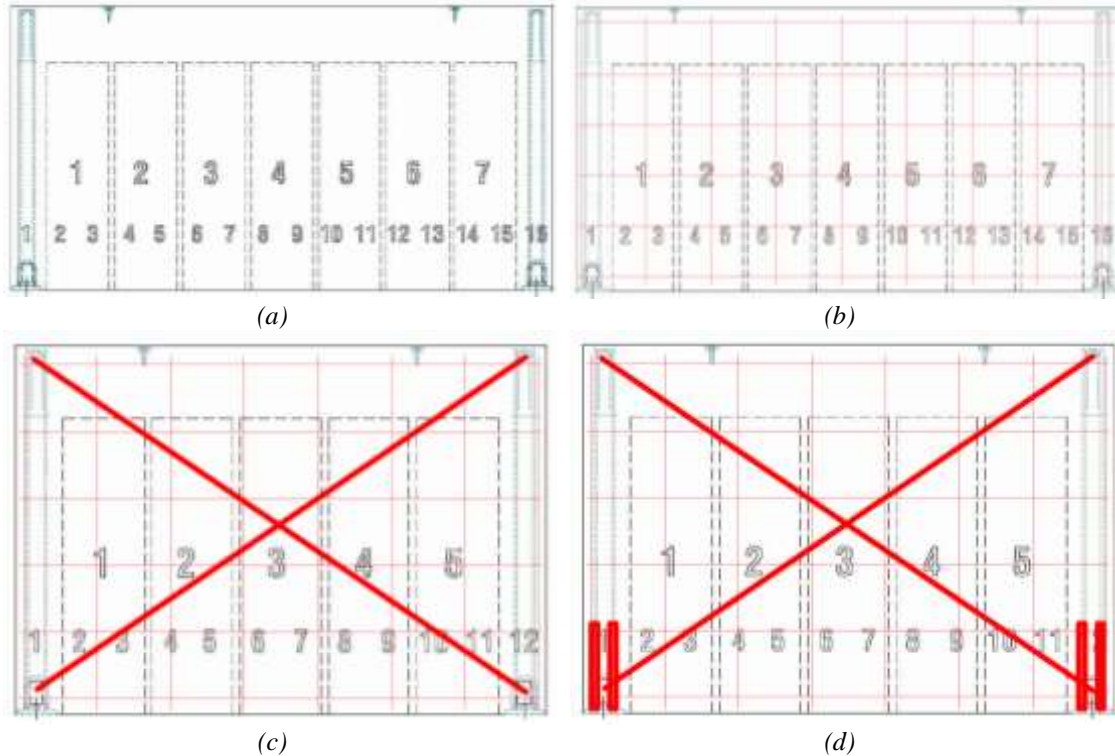


Figure 2. Geometry and schematic reinforcement details of the tested wall specimens: (a) Wall 1 without shear reinforcement; (b) Wall 2 with welded wire meshes; (c) Wall 3 with additional diagonal bars; (d) Wall 4 with additional sleeves on longitudinal bars.

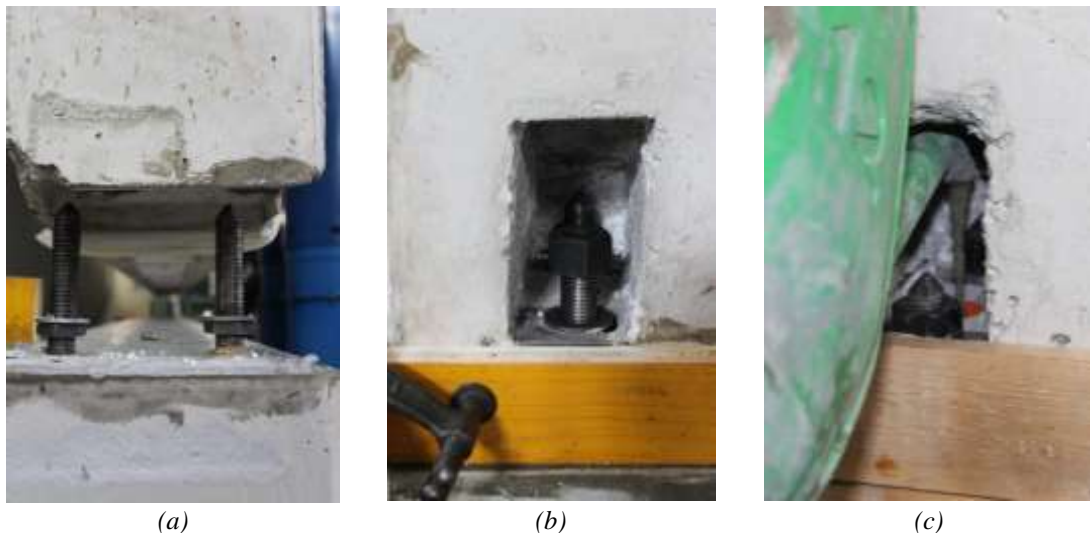


Figure 3. Phases of joint assemblage: (a) inserting the wall element into the bar anchors of the foundation element and mechanically regulating of the verticality acting on the bottom shallow nuts; (b) screwing the top nut and installation of local formworks; (c) pouring the high-strength non-shrinking completion mortar.

upper nuts for safety in transient phase; (IV) regulation of verticality acting from the bottom nuts; (V) tightening of the upper nuts (a special torsional wrench has been used to tighten the inner connection due to the small room); (VI) installation of the temporary local mold; (VII) pouring of the high-strength non-shrinking mortar; (VIII) removal of the local mold after mortar ageing. The specimens are made with concrete class C45/55. Grade B450C steel reinforcement for the bars and grade B450A for the welded wire meshes. Ruredil Exocem G1 mortar was used for joint completion.

3 TEST SETUP AND PROTOCOL

The test setup is shown in Figures 4 and 5. The foundation element is connected to the base strong beam of the test rig through a bolted connection made by tightening 12 M20 bolts (6 per side) through holes provided into the base beam and into sockets embedded into the foundation element. The axial displacement of the foundation beam is further hampered by steel angles leaned on the edges. The load is applied by a double-hinged electric-mechanical actuator with a 1000 kN capacity, placed at the top of the braced frame of the test rig with its axis at only few centimetres from the top of the wall element. The load is transmitted by direct contact when pushing and by direct contact on the opposite side when pulling. A rigid transverse steel beam has been installed at the top wall edge on the opposite side of the actuator and connected to it through Dywidag bars running externally to the concrete wall mock-up. To each bar was a 10 kN pre-tension was applied. Potential modification of the wall behaviour under imposed horizontal displacement due to this clamping action has been investigated by comparing the results of two similar wall specimens (Wall 3 and Wall 4) where Wall 3 has been subjected to bi-lateral cyclic displacement through the application of the clamping device, and Wall 4 has been subjected to uni-lateral cyclic displacement with the direct transmission of the load through pushing only. The results showed no relevant difference. Lateral follower spheres acting over an external contour frame restrain the out-of-plane displacement of the actuator.

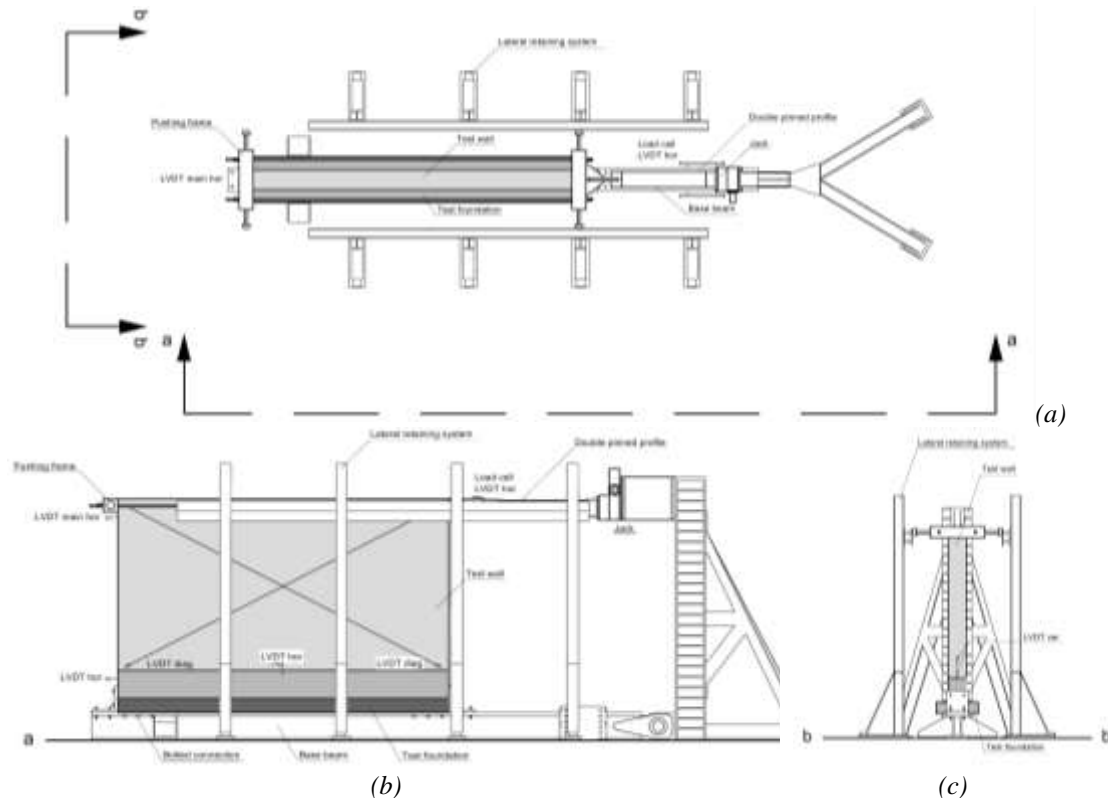


Figure 4. Test setup: (a) top view; (b) side view; (c) front view.

The actuator is provided with a load cell, whereas horizontal LVDTs are installed at the top of the wall (one facing the wall and one connected to the actuator) and at the bottom (one at the interface between wall and foundation beam and one between foundation beam and lab strong floor). Diagonal wire LVDTs are installed on one side of the wall panel. Each test was first conducted in load control up to about one third of the expected ultimate load with one cyclic repetition to identify the elastic stiffness. Afterwards, the control has been switched to displacement mode (the top displacement of the wall was assumed as a control variable), and a cyclic test was performed with three cyclic repetitions at each displacement amplitude starting from 0.3 mm and gradually increasing it by 50% up to failure. Wall 4 was tested cyclically in one direction only with the aim to verify a possible influence of the top clamp device on the structural behavior through the comparison with the similar specimen Wall 3 tested bi-directionally.

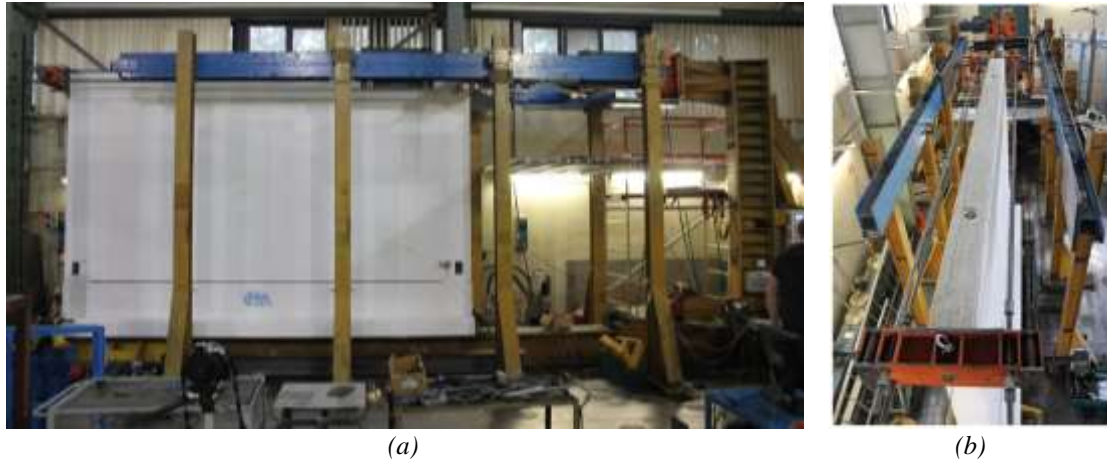


Figure 5. Pictures of the test setup: (a) side view; (b) top/front view.

Table 1. Main experimental data.

Specimen	K_{el} panel [kN/mm]	K_{el} global [kN/mm]	δ_u^* [mm]	Δ_u^* [%]	P_u [kN]	Failure Mode
Wall 1	380	210	5.0	0.20	299	Tension shear
Wall 2	520	350	7.9	0.32	472	Mixed
Wall 3	240~290	180~230	27.6	1.10	435	Sliding shear
Wall 4	280	220	20.7	0.83	439	Sliding shear

* The ultimate displacement is evaluated after a load decrement of 15% after peak

4 EXPERIMENTAL RESULTS

The main test results are summarized in Table 1. The contribution of the deformation concentrated into the wall-foundation connections is crucial for the correct estimation of the elastic stiffness, ranging in the analyzed cases from an additional 20 to 40% of the stiffness of the wall panel only. The hysteretic behavior of the specimens is shown in Figure 6 with reference to both global displacement and wall panel displacement only. Figures 7 and 8 show the crack pattern at the end of the tests.

Wall 1, without shear reinforcement, shows a non-linear hysteretic behavior characterized by pinching and ending with a sudden strength loss (Figure 6a), corresponding to the opening of the critical crack, which is found to be aligned orthogonally to the diagonal tie (Figures 7a and 8a). This failure corresponds to the axial failure of the diagonal tie and can be classified as tension-shear failure.

Wall 2, with welded wire meshes placed as shear reinforcement, shows a similar hysteretic behavior although the failure occurred at a higher ultimate load (+58%) and displacement (+60%), where the ultimate displacement is evaluated after a load decrement of 15%

after peak (Figure 6b). Despite cracks develop in the direction orthogonal to the diagonal tie, the presence of the meshes allowed a stable response to be obtained, and failure occurred for sudden sliding of the wall panel over the foundation with large cracks opening also in the diagonal tie (Figures 7b and 8b). Therefore, the failure mode is classified as mixed in between tension and sliding shear. Relevant cracks opened in the foundation element as well, with the critical crack identifying a concrete cone failure on the compressed side. It can be clearly seen from the wall displacement in Figure 6b that a relevant hysteresis occurs in the wall-to-foundation connections at the interface, associated with yielding of the mesh steel.

Wall 3, with additional diagonal reinforcement, does not show diagonal cracking, with a structural behavior characterized by contemporary progressive damaging of the wall/foundation interface and yielding of the longitudinal rebars in bending. The first mechanism provides the pinching behavior observed in Figure 6c. The displacement capacity is much larger than the previous walls, with more than 1% of ultimate drift. The critical cracks at failure (Figure 8c) are pseudo-horizontal in the tensioned side along the wall/foundation interface (Figure 7c) and inclined into the foundation in the compressed side with the detachment of the edge concrete cone (Figure 7d).

Wall 4, with debonding sleeves on the longitudinal rebars, shows a behavior (Figure 6d) quite similar to Wall 3, although the applied load is cycled on one side only. Sliding shear failure occurred prior to longitudinal vertical rebars failure in tension.

The mean vertical strain histories measured at a base of 250 mm at both edges of the wall panel right above the foundation are shown in Figure 9 for Wall 2 and Wall 3, where the alternate peaks correspond to the tension cycles imposed by the top horizontal displacement. The behavior of Wall 2 is characterized by relevant strain variations which are influenced by the opening of shear cracks and oscillate around a small residual strain. On the contrary, the progressive plasticization of the vertical bars in Wall 3 can be observed by looking at the cumulated plastic strain tendency, increasing with the displacement.

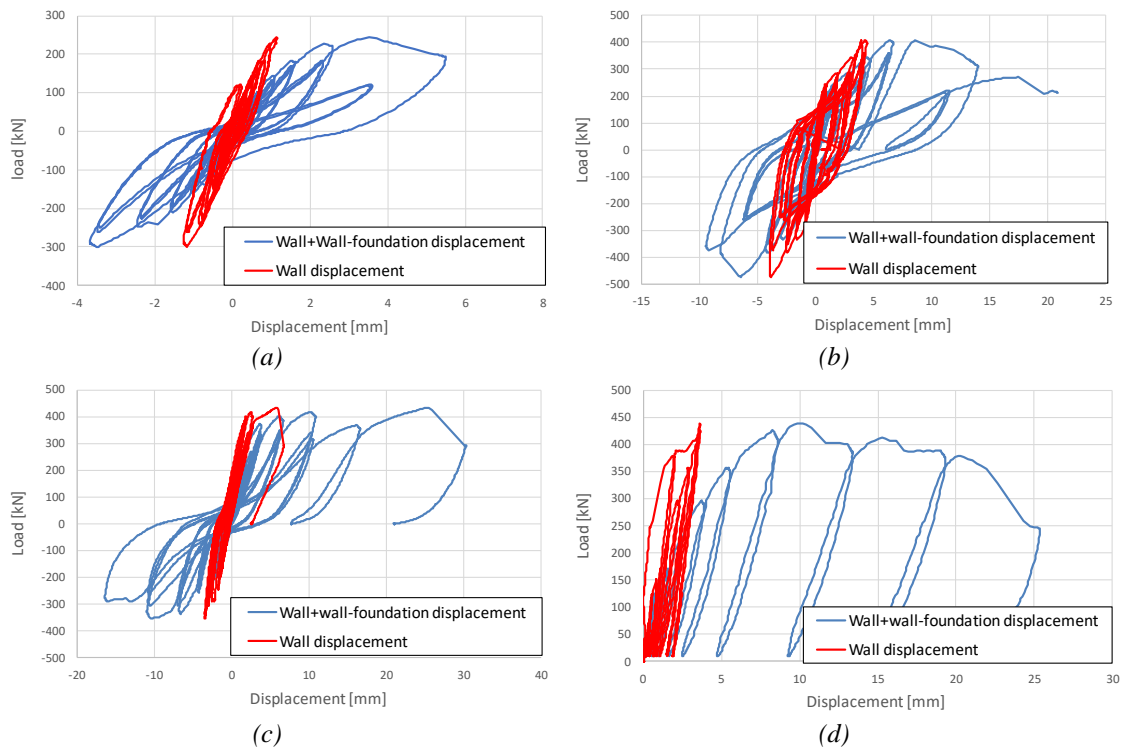


Figure 6. Load vs displacement curves: (a) Wall 1; (b) Wall 2; (c) Wall 3; (d) Wall 4.

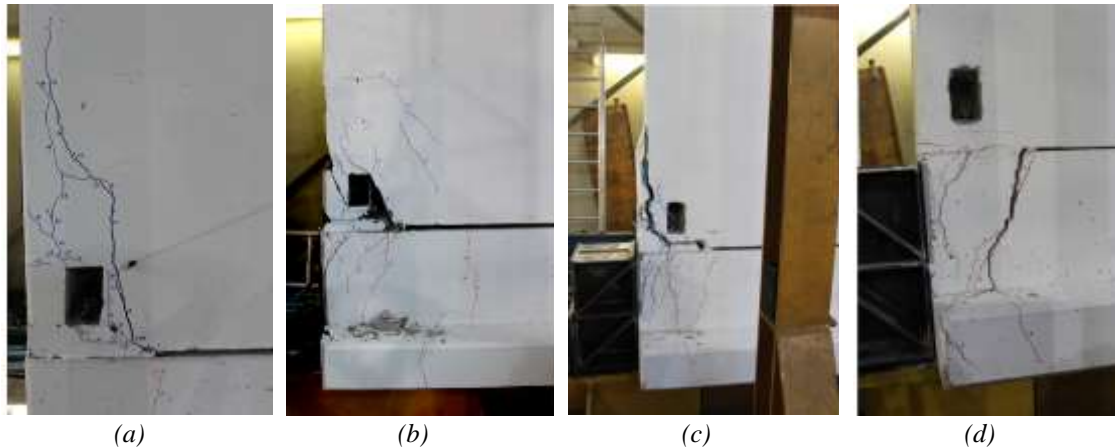


Figure 7. Failure crack pattern: (a) Wall 1 – tensioned side; (b) Wall 2 – tensioned side; (c) Wall 3 – tensioned side; (d) Wall 4 – compressed side.

5 ENGINEERING INTERPRETATION

The experimental programme showed two shear failure mechanisms: tension shear and sliding shear. In the following, the shear strength of the different specimens according to the above-cited failure modes is interpreted and calculated with the aid of formulations existing in literature. Regarding tension shear, this mechanism of failure is interpreted with a strut & tie model as per Figure 10a. The elements are checked both in compression and in tension. Failure is considered attained when the first element fails. The dimension of the diagonal strut/tie is strictly influenced by the value of the diffusion angle β (Figure 10b). The default value considered by the designers was 15° on the safe side, due to lack of experimental evidence. This angle has been set to 24° after the test observations.

Regarding the sliding shear failure strength, it is supposed to be associated to 3 contemporary mechanisms: a) friction force at wall/foundation interface (EC2); b) dowel effect provided by the longitudinal reinforcement at tensioned side (formulation by Toniolo in EN 25377); c) concrete cone formation into the foundation (formulation by Toniolo in EN 25377 and Zoubek *et al.*, 2015). It is worth remarking that the formulation by Zoubek, while providing a better estimation of the influence of the steel reinforcement crossing the cone surface, does not account for axial influence over shear strength of dowels, which is not relevant for the case of pinned beam-to-column connections, but which is relevant for the case under study. Thus, the dowel strength on the steel side has been corrected using the formulation by Toniolo in EN 25377, which accounts for this effect. In the shear strength diagrams of Figure 11, the failure can be identified when the failure line crosses one of the curves corresponding to each of the above-described failure modes. The comparison of the experimental strength with that found analytically is satisfactory both in terms of failure mode identification and in terms of shear strength.

CONCLUSIONS

The experimental programme allowed to assess the possible failure modes of the wall system under investigation, which have been identified as tension-shear failure with critical diagonal tie cracking and sliding shear failure with pseudo-horizontal critical cracking at tensioned side and concrete cone failure of lower element at compressed side. It was observed that the walls with additional diagonal shear reinforcement fail under sliding shear. However, sliding shear strength is strongly depending upon friction mechanism, which is a function of the axial load. The tested walls had no additional axial load except for their own weight, but this is a condition which is rarely found in the practice, where these walls are used as bearing walls. The tension-shear failure has been better defined calibrating the diffusion angle of the strut/tie against the test observation and interpreting the shear resisting mechanism of the wall panel with a strut & tie model.

The engineering interpretation of the results provided a good matching of both strength values and failure mode identification. Furthermore, the correct functioning of the Kaptor connection device in allowing plastic deformation of the longitudinal reinforcing bars has been assessed.

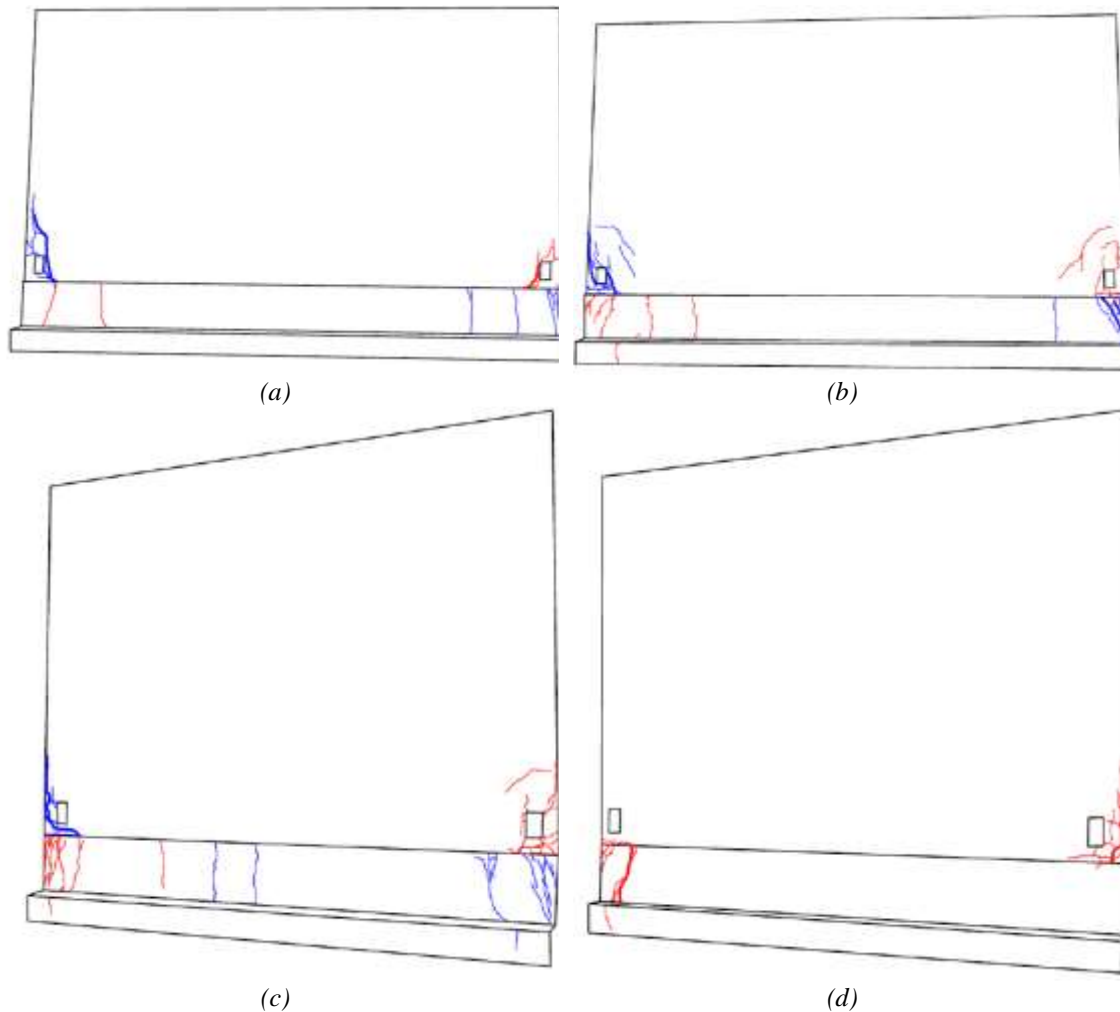


Figure 8. Crack pattern at end of testing: (a) Wall 1; (b) Wall 2; (c) Wall 3; (d) Wall 4.

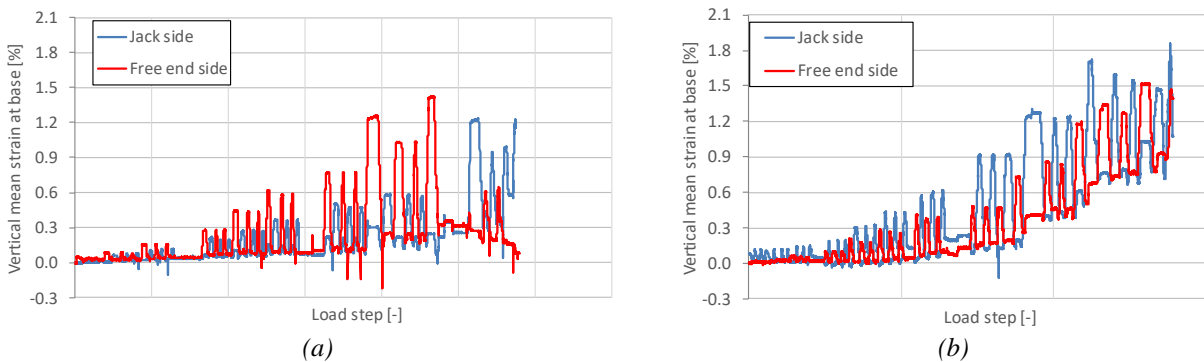


Figure 9. Vertical mean strain evolution at panel base over a measure base of 250 mm: (a) Wall 2; (b) Wall 3.

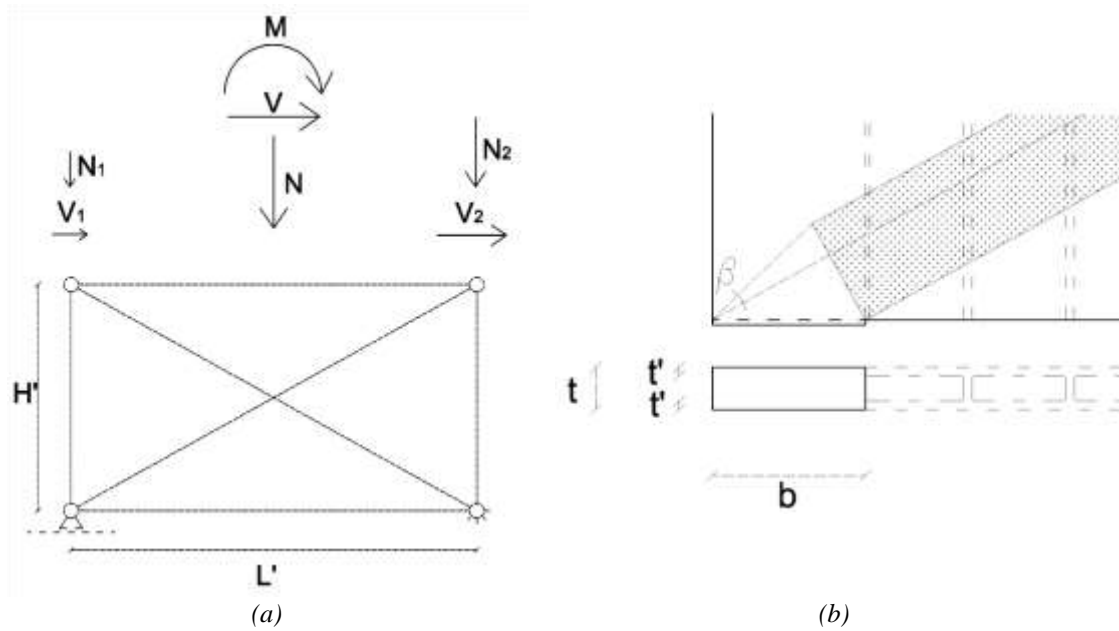


Figure 10. (a) Strut and tie model; (b) Default angle of diffusion.

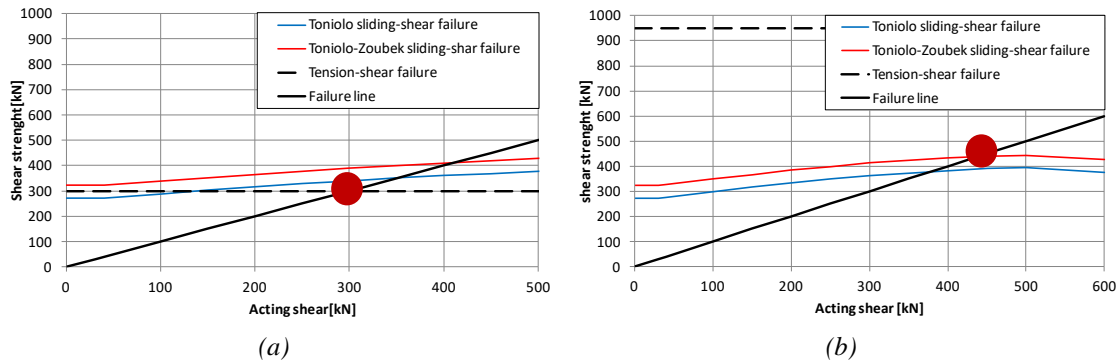


Figure 11. Strength diagrams for: (a) Wall 1; (b) Wall 3 and Wall 4.

ACKNOWLEDGEMENTS

The activity illustrated in the paper frames into a wider research program focused on an innovative dry-assembled precast system for residential constructions named Domus Dry[®] patented by DLC Consulting S.r.l. of Milan and received main funding from the programme “Brevetti+” (g.u. 179 of 02/08/2011). The company TreColli S.p.a. located in Carrosio (AL) is gratefully acknowledged for the production of the elements, especially Eng. Repetto and Mr. Tabacchin. The lab technicians Eng. Vazzana and Mr. Antico are acknowledged for their assistance to assemblage of the setup and performance of the tests.

REFERENCES

- Bora C., Oliva M.G., Nakaki S.D. and Becker R. (2007). Development of a precast concrete shear-wall system requiring special code acceptance. *PCI Journal*, January-February, 1-14.
- Chu M., Liu J. and Sun Z. (2017). Experimental study on mechanical behaviors of new shear walls built with precast concrete hollow moulds. *Eur. J. Env. Civ. Eng.*, published online.
- Dal Lago A. (2002). Domus, un nuovo sistema per il rilancio della prefabbricazione residenziale e terziaria. *14th CTE Congress*, Mantova, Italy, November 7-9.
- Dal Lago A. (2006). Sistema di prefabbricazione di pareti a fori verticali. *16th CTE Congress*, Parma, Italy, November 9-11.

- Dal Lago A. (2012a). Il sistema Domus Dry per un'edilizia industrializzata montata a secco. *19th CTE Congress*, Bologna, Italy, November 8-10.
- Dal Lago A. (2012b). Il sistema Kaptor per realizzare collegamenti in zona sismica. *ACI Italy Chapter Workshop: connections in precast structures*, Bergamo, Italy, October 5.
- Dal Lago B. and Dal Lago A. (2018). New precast constructions for integrated complex urban interventions. *BFT International*, V.84, No.4, 72-80.
- Dal Lago B., Dal Lago A., Franceschelli F. (2016). Innovation for smart industrial housing. *Concrete Plant International*, V.2, 298-300.
- Dal Lago B, Muhaxheri M. and Ferrara L. (2017). Numerical and experimental analysis of an innovative lightweight precast concrete wall, *Engineering Structures*, V.137, 204-222.
- Dal Lago B., Toniolo G. and Lamperti Tornaghi M. (2016). Influence of different mechanical column-foundation connections on the seismic performance of precast structures. *Bulletin of Earthquake Engineering*, V.14, No.12, 3485-3508.
- EN 1992-1-1. (2005). Eurocode 2: Design of concrete structures - Part 1-1: General rules and rules for buildings. European Institute for Standardization, Brussels, Belgium.
- EUR 25377 EN (2012). Design guidelines for connections of precast structures under seismic action. *JRC Scientific and Policy Report*, P. Negro and G. Toniolo Eds.
- Hamid N.H. and Mander J.B. (2010). Lateral seismic performance of multipanel precast hollowcore walls. *Journal of Structural Engineering*, ASCE, V.136, No.7, 795-804.
- Negro P., Bournas D.A. and Molina F.J. (2013). Pseudodynamic Tests on a full-scale 3-storey precast concrete building: global response. *Engineering Structures*, V.57, 594-608.
- Xiong C., Chu M., Liu J. and Sun Z. (2018). Shear behavior of precast concrete wall structure based on two-way hollow-core precast panels. *Engineering Structures*, V.176, 74-89.
- Xu G. and Li A. (2019). Research on the response of concrete cavity shear wall under lateral load. *Tall and Special Buildings*, V.28, No.3, e1577.
- Zoubek B., Fischinger M. and Isakovic T. (2015). Estimation of the cyclic capacity of beam-to-column dowel connections in precast industrial buildings. *Bulletin of Earthquake Engineering*, V.13, No.8, 2145-2168.